

Non-collinear and non-degenerate polarization-entangled photon generation via concurrent type-I parametric downconversion in PPLN

Hugues Guillet de Chatellus*, Alexander V. Sergienko, Bahaa E. A. Saleh and Malvin C. Teich

Quantum Imaging Laboratory,
Department of Electrical & Computer Engineering and Department of Physics
Boston University, 8 Saint Mary's Street
Boston, Massachusetts 02215

* Laboratoire de Spectrométrie Physique, CNRS-Université Joseph Fourier
140 avenue de la physique, BP 87
38402 Saint Martin d'Hères, France

AlexSerg@bu.edu

Giovanni Di Giuseppe

Department of Physics
University of Camerino, Via Madonna delle Carceri, 9
I-62032 Camerino, Italy

Abstract: A periodically poled lithium niobate (PPLN) crystal has been used as an efficient source of non-collinearly generated polarization-entangled photon pairs at 810 and 1550 nm. The PPLN crystal was endowed with a specially designed poling pattern and the entangled photons were generated via the nonlinear optical process of spontaneous parametric down conversion (SPDC). A novel design based on overlapping two concurrent type-I quasi-phase-matching structures in a single PPLN crystals produced correlated pairs of alternatively polarized photons in largely separated spectral regions. The phase of the resulting two-photon state is directly linked to parameters of the nonlinear grating. Continuous tunability of the generated Bell state, from Φ^+ to Φ^- , has been demonstrated by translating a slightly wedged crystal perpendicular to the pump beam.

© 2006 Optical Society of America

OCIS codes: (270.0270) Quantum optics; (190.4410) Nonlinear optics, parametric processes.

References and links

1. D. N. Klyshko, *Photons and Nonlinear Optics*, Gordon and Breach (New York, 1988).
2. Z. Y. Ou and L. Mandel, "Violation of Bell's inequality and classical probability in a two-photon correlation experiment," *Phys. Rev. Lett.* **61**, 50-53 (1988).
3. Y. H. Shih and C. O. Alley, "New type of Einstein-Podolsky-Rosen-Bohm experiment using pairs of light quanta produced by optical parametric down conversion," *Phys. Rev. Lett.* **61**, 2921-2924 (1988).
4. A. Migdall, R. Datla, A. V. Sergienko, and Y. H. Shih, "Absolute detector quantum efficiency measurements using correlated photons", *Metrologia*, **32**, 479-483 (1995).
5. D. Branning, A. L. Migdall, and A. V. Sergienko, "Simultaneous measurement of group and phase delay between two photons," *Phys. Rev. A* **62**, 63808 (2000).

6. T. B. Pittman, Y. H. Shih, D. V. Strekalov, and A. V. Sergienko, "Optical imaging by means of two-photon quantum entanglement", *Phys. Rev. A* **52**, R3429-3432 (1995).
7. A. F. Abouraddy, B. E. A. Saleh, A. V. Sergienko, and M. C. Teich, "Entangled-photon Fourier optics," *J. Opt. Soc. Am. B* **19**, 1174-1184 (2002).
8. M. B. Nasr, B. E. A. Saleh, A. V. Sergienko, and M. C. Teich, "Dispersion-cancelled and dispersion-sensitive quantum optical coherence tomography," *Opt. Express* **12**, 1353-1362 (2004).
9. J. C. Howell, R. S. Bennink, S. J. Bentley, and R. W. Boyd, "Momentum-position realization of the Einstein-Podolsky-Rosen paradox using spontaneous parametric downconversion", *Phys. Rev. Lett.* **92**, 210403 (2004).
10. D. Bouwmeester, A. K. Ekert et al. (Eds.), *The Physics of Quantum Information*, Springer (New York, 1999).
11. D. Bouwmeester, J.-W. Pan, K. Mattle, M. Eibl, H. Weinfurter, and A. Zeilinger, "Experimental quantum teleportation," *Nature* **390**, 575 (1997).
12. D. Boschi, S. Branca, F. De Martini, L. Hardy, and S. Popescu, "Experimental realization of teleporting an unknown pure state via dual classical and Einstein-Podolsky-Rosen channels," *Phys. Rev. Lett.* **80**, 1121-1125 (1998).
13. K. Mattle, H. Weinfurter, P. G. Kwiat, and A. Zeilinger, "Dense coding in experimental quantum communications," *Phys. Rev. Lett.* **76**, 4656 (1996).
14. W. Tittel, J. Brendel, H. Zbinden, and N. Gisin, "Quantum cryptography using entangled photons in energy-time Bell states," *Phys. Rev. Lett.* **84**, 4737-4740 (2000).
15. T. Jennewein, C. Simon, G. Weihs, H. Weinfurter, and A. Zeilinger, "Quantum cryptography with entangled photons," *Phys. Rev. Lett.* **84**, 4729-4732 (2000).
16. A. V. Sergienko, ed., *Quantum Communications and Cryptography*, CRC Press, Taylor & Francis Group (New York, 2005).
17. P. G. Kwiat, K. Mattle, H. Weinfurter, A. Zeilinger, A. V. Sergienko, and Y. Shih, "New high-intensity source of polarization-entangled photon pairs," *Phys. Rev. Lett.* **75**, 4337-4341 (1995).
18. M. Fiorentino, C. E. Kuklewicz, and F. N. C. Wong, "Source of polarization entanglement in a single periodically poled KTiOPO₄," *Opt. Express* **13**, 127-135 (2005).
19. P. G. Kwiat, E. Waks, A. G. White, I. Appelbaim, and P. H. Eberhard, "Ultrabright source of polarization entangled photons," *Phys. Rev. A* **60**, R773-776 (1999).
20. M. Pelton, P. Marsden, D. Ljunggren, M. Tengner, A. Karlsson, A. Fragemann, C. Canalias, and F. Laurell, "Bright, single-spatial-mode source of frequency non-degenerate, polarization-entangled photon pairs using periodically poled KTP," *Opt. Express* **12**, 3573-3580 (2004).
21. C. E. Kuklewicz, M. Fiorentino, G. Messin, F. N. C. Wong, and J. H. Shapiro, "High-flux source of polarization-entangled photons from a periodically-poled KTiOPO₄ parametric down-converter," *Phys. Rev. A* **69**, 013807 (2004).
22. F. König, E. J. Mason, F. N. C. Wong and M. A. Albota, "Efficient and spectrally bright source of polarization-entangled photons," *Phys. Rev. A* **71**, 033805 (2005).
23. J. A. Armstrong, N. Bloembergen, J. Ducuing, and P. S. Pershan, "Interactions between light waves in a nonlinear dielectric," *Phys. Rev.* **127**, 1918 (1962).
24. L. E. Myers, R. C. Eckart, M. M. Fejer, R. L. Byer, W. R. Rosenberg, and J. W. Pierce, "Quasi-phasematched optical parametric oscillators using bulk periodically poled LiNbO₃," *J. Opt. Soc. Am. B* **12**, 2102 (1995).
25. G. D. Miller, R. G. Batchko, W. M. Tulloch, D. R. Weise, M. M. Fejer, and R. L. Byer, "42% Efficient single-pass cw second-harmonic generation in periodically poled LiNbO₃," *Opt. Lett.* **22**, 1834 (1997).
26. S. Tanzilli, H. De Riedmatten, W. Tittel, H. Zbinden, P. Baldi, M. De Micheli, D. B. Ostrowski, and N. Gisin, "Highly efficient photon-pair source using periodically poled lithium niobate waveguide," *Electron. Lett.* **37**, 26-28 (2001).
27. C. Elliott, "The DARPA quantum network," ArXiv, quant-ph/0412029.
28. S. Carrasco, J. P. Torres, L. Torner, A. Sergienko, B. E. A. Saleh, and M. C. Teich, "Spatial-to-spectral mapping in spontaneous parametric down-conversion" *Phys. Rev. A* **70**, 043817 (2004).
29. G. D. Miller, "Periodically poled lithium niobate: Modeling, fabrication, and nonlinear-optical performance," Ph.D. dissertation (Stanford University, July 1998).
30. H. Guillet de Chatellus, G. Di Giuseppe, A. V. Sergienko, B. E. A. Saleh, M. C. Teich, "Engineering entangled-photon states using two-dimensional PPLN crystals," *Proc. SPIE* **5456**, 11 (2004).

1. Introduction

Spontaneous parametric downconversion (SPDC) [1] has been widely used as a source of correlated and entangled photon pairs in many quantum optics experiments. Applications of such optical states include tests of basic quantum mechanics [2, 3], precise optical measurements [4, 5], quantum imaging [6, 7, 8, 9], and quantum information [10], among others. The encoding of quantum information using polarization has served as a reliable technique for implementing

such nonclassical effects as quantum teleportation [11, 12], quantum dense coding [13], and secure quantum key distribution (QKD) [14, 15, 16].

Practical quantum cryptography is expected to benefit from the availability of a compact and efficient source of polarization entanglement between photons whose frequencies are well separated, particularly when one of the wavelengths falls in the telecommunication window near 1550 nm and the other lies in the visible region [16]. The entangled-photon QKD protocol relies on the joint (coincidence) detection of the photon pair at two spatially separated nodes. The benefit arises because of the superior performance of Si photon-counting detectors in the visible region relative to InGaAs detectors in the infrared. In particular, double-wavelength entanglement enhances the overall efficiency of the entangled-photon QKD scheme by allowing the visible photon to be detected locally, with a low-noise detector at Alice's node, while the infrared photon is transmitted to Bob's site via a low-loss optical fiber. The detection of the visible photon effectively serves to herald the arrival of its infrared partner at the remote node, which has a noisier InGaAs detector, thus allowing the observer to narrow the detection-time window and thereby increase the signal-to-noise ratio for the overall process.

Various efforts to construct compact and efficient sources of polarization entanglement suitable for practical use have been reported over the past decade. Historically, the most commonly used scheme makes use of type-II SPDC in a bulk beta-barium borate (BBO) crystal; this provides polarization entanglement along two particular non-collinear directions in space [17]. However, this approach suffers from a low efficiency of entangled-pair production because of the poor overlap of the two orthogonally polarized SPDC cones. The group-velocity mismatch between the two orthogonal polarizations in the birefringent nonlinear crystal destroys the timing indistinguishability of two photons; this must be restored by making use of an additional birefringent element to compensate for the longitudinal walk-off acquired inside the nonlinear material.

The overlap of the two orthogonally polarized SPDC cones can be improved by pumping the crystal in the direction of one of its principal axes, which generates entanglement around a whole revolution cone [18]. However, the use of type-II phase matching to generate polarization entanglement with this approach is restricted to the degenerate case, where the frequencies of the signal and idler photons are coincident.

The need for additional compensation optics can be avoided by using type-I SPDC, for which temporal walk-off is negligible. A polarization-entangled state can be engineered by making use of fully overlapping correlated-photon outcomes from separate nonlinear interactions in two thin type-I nonlinear crystals placed immediately adjacent to each other; downconversion with orthogonal polarizations emerges from the crystal pair when pumped by a single beam polarized at 45° [19]. The photon pairs are generated along any set of directions that are symmetric with respect to the axis of the pump beam, and this leads to high efficiency. The close spacing of the crystals renders the otherwise independent processes indistinguishable, thus creating a polarization-entangled state. A principal limitation of this approach is that the nonlinear crystals must be rather thin to preserve the indistinguishability of pairs in the non-collinear case. Also, an additional birefringent plate must be placed in the path of the pump beam to tune the phase of a Bell-state. An extension of this approach that makes use of two orthogonally oriented PPKTP crystals has led to the collinear generation of nondegenerate polarization-entangled pairs [20]. Instead of pumping two nonlinear crystals with a single pump beam, it is also possible to produce polarization entanglement by pumping a single nonlinear crystal with two counter-propagating pump beams [21, 22]. However, such implementations require additional optics. External optical elements are also often required to spatially separate the photons of a pair because, traditionally, nonlinear interactions in PPLN utilize a collinear geometry of interacting waves. Finally, the fine tuning of an output state, and the switching from one polarization Bell-

state to another, requires the insertion of auxiliary birefringent elements in the outgoing beams.

Is it possible to create a compact single-crystal source, pumped by a single beam, that generates polarization-entangled photon pairs, with well separated frequencies in a non-collinear geometry, that does not require additional optics for tuning the output state? We demonstrate, both theoretically and experimentally, that a specially engineered periodically poled crystal (PPC) can serve as just such a source when suitably prepared.

The organization of the remainder of this paper is as follows. We first demonstrate the possibility of designing a poling pattern in a PPC that allows the generation of polarization-entangled states via the overlap of two different, but concurrently existing, type-I nonlinear interactions in the same crystal. The resulting two-photon state is then determined; its phase is shown to be directly linked to the profile of the periodic nonlinearity in the PPC. This suggests the possibility of tuning the phase of the outgoing two-photon state by forming a wedged PPC and translating it in the field of the pump laser. While we have established that this technique is applicable for an arbitrary periodically poled nonlinear material, we select periodically poled lithium niobate (PPLN) for the first demonstration. In particular, we generate non-degenerate polarization-entangled photon pairs at 810 and 1550 nm directly from a single PPLN crystal with two overlapping type-I parametric interactions. We examine the spatial and spectral characteristics of the emerging photons that are required for indistinguishability between the two contributing processes. A Bell-state measurement that demonstrates the nonclassical behavior of the ensuing two-photon state is reported. Finally, we demonstrate the tuning of the state from Φ^+ to Φ^- by a simple translation of the crystal.

2. Generation of entanglement in a PPC: Theoretical considerations

2.1. Two-photon state produced by SPDC in a PPC

Periodically poled crystals, which make use of quasi-phase matching [23], are suitable for achieving parametric oscillation [24], frequency up-conversion [25] and, in a conventional configuration, SPDC [18, 20, 21, 26]. Here we provide a general description of SPDC in a PPC that elucidates the design of our special poling patterns.

We consider the simple case of a plane-wave pump traveling along the x direction in a nonlinear medium that occupies a volume V between $x = 0$ and $x = L$, which is periodically poled with spatial period Λ . As always, the components of the second-order susceptibility tensor can be written as

$$\chi_{ijk}^{(2)}(\mathbf{r}) = \sum_{\mathbf{q}} \tilde{\chi}_{ijk}^{(2)}(\mathbf{q}) e^{i\mathbf{q}\cdot\mathbf{r}}, \quad (1)$$

where the summation is over all spatial wavevectors \mathbf{q} associated with the Fourier spectrum of the spatial profile of the periodically modulated nonlinearity. In a one-dimensional PPC, \mathbf{q} is directed along x . The Fourier transform of the nonlinear profile can be reduced to

$$\tilde{\chi}_{ijk}^{(2)}(\mathbf{q}) = \frac{1}{\Lambda} \int_{-\Lambda/2}^{+\Lambda/2} dx \chi_{ijk}^{(2)}(x) e^{-i\mathbf{q}\cdot\mathbf{r}}. \quad (2)$$

The finiteness of the nonlinear medium is accounted for by the integration over the volume of the crystal. The wavevectors \mathbf{q} are the spatial harmonics of the modulation. In the general case of an infinite PPC, they can be written as $\mathbf{q} = n \cdot \mathbf{q}_0$ where $|\mathbf{q}_0| = q_0 = 2\pi/\Lambda$ is an elementary vector of the reciprocal lattice, and n is an integer.

Accommodating the various components of the second-order nonlinear tensor, the two-photon state produced by SPDC can be written as [1]

$$|\psi^{(2)}\rangle \sim \int_V d\mathbf{r} \int dt \sum_{\text{tensor}} \chi_{psi}^{(2)}(x) \hat{E}_p^+(\mathbf{r}, t) \hat{E}_s^-(\mathbf{r}, t) \hat{E}_i^-(\mathbf{r}, t) |\text{vac}\rangle, \quad (3)$$

where \widehat{E}_s^- and \widehat{E}_i^- are the field operators of the signal and idler, respectively:

$$\widehat{E}_s^-(\mathbf{r}, t) = \int d\omega_s \sqrt{\frac{\omega_s}{n_s(\omega_s)}} E_s e^{-i\mathbf{k}_s(\omega_s)\cdot\mathbf{r}} e^{i\omega_s t} a_s^+(\omega_s, \mathbf{k}_s(\omega_s)), \quad (4)$$

$$\widehat{E}_i^-(\mathbf{r}, t) = \int d\omega_i \sqrt{\frac{\omega_i}{n_i(\omega_i)}} E_i e^{-i\mathbf{k}_i(\omega_i)\cdot\mathbf{r}} e^{i\omega_i t} a_i^+(\omega_i, \mathbf{k}_i(\omega_i)). \quad (5)$$

The classical pump field is specified by the complex amplitude

$$E_p^+(\mathbf{r}, t) = \int d\omega_p \sqrt{\frac{\omega_p}{n_p(\omega_p)}} E_p e^{i\mathbf{k}_p(\omega_p)\cdot\mathbf{r}} e^{-i\omega_p t}. \quad (6)$$

The quantities E_p , E_s , and E_i represent the spatial modes of the pump, signal, and idler fields respectively. The polarizations of the three photons are denoted as p , s , and i , respectively; they can be ordinary (o) or extraordinary (e). The magnitude of the pump wavevector is $|\mathbf{k}_p(\omega_p)| = k_p(\omega_p) = 2\pi n_p(\omega_p) \omega_p / c$ where ω_p is the pump frequency and $n_p(\omega_p)$ is the refractive index of a p -polarized monochromatic wave of frequency ω_p in the nonlinear crystal. Similar relations can be written for the signal and idler waves.

In the case of a plane-wave, the SPDC state becomes

$$|\psi^{(2)}\rangle \sim \int d\omega_s d\omega_p \delta(\omega_p - \omega_s - \omega_i) \left(\sum_{\text{tensor}} \sum_{n=-\infty}^{n=+\infty} \frac{\widetilde{\chi}_{psi}^{(2)}(n\mathbf{q}_0)}{\sqrt{n_p(\omega_p) n_s(\omega_s) n_i(\omega_i)}} \right) \quad (7)$$

$$\times \int_V d\mathbf{r} e^{i(\mathbf{k}_p(\omega_p) - \mathbf{k}_s(\omega_s) - \mathbf{k}_i(\omega_i) - n\mathbf{q}_0)\cdot\mathbf{r}} |1_{\omega_s, \mathbf{k}_s(\omega_s)}\rangle |1_{\omega_i, \mathbf{k}_i(\omega_i)}\rangle.$$

The double summation suggests the possibility of producing at least two independent photon pairs in the same spectral (ω_s, ω_i) and spatial ($\mathbf{k}_s(\omega_s), \mathbf{k}_i(\omega_i)$) modes, and therefore to the possibility of constructing an entangled state, provided that energy and momentum are conserved. As an example, we consider the case where the nonlinear tensor has two nonvanishing components, $\chi_{eee}^{(2)}$ and $\chi_{eoo}^{(2)}$. The crystal can then be pumped by an e -polarized pump beam to produce the maximally polarization-entangled Bell state

$$|\Phi\rangle = (|e, e\rangle + e^{i\phi} |o, o\rangle) / \sqrt{2}, \quad (8)$$

where the first term is enabled by the $\chi_{eee}^{(2)}$, and the second by the $\chi_{eoo}^{(2)}$, components of the nonlinear tensor, respectively.

Several conditions must be fulfilled for a polarization-entangled state to be synthesized:

1. Energy must be conserved: $\omega_p = \omega_s + \omega_i$.
2. Momentum must be conserved, i.e., a pair of integers n_{ee}, n_{oo} must exist that satisfy the quasi-phase matching conditions:

$$\begin{aligned} \mathbf{k}_e(\omega_p) - \mathbf{k}_e(\omega_s) - \mathbf{k}_e(\omega_i) &= n_{ee}\mathbf{q}_0 \\ \mathbf{k}_e(\omega_p) - \mathbf{k}_o(\omega_s) - \mathbf{k}_o(\omega_i) &= n_{oo}\mathbf{q}_0. \end{aligned} \quad (9)$$

3. A spatial mode of the e -polarized signal photon of a pair must overlap with the spatial mode of the o -polarized signal photon of the same frequency from the second interaction, and vice versa (see Fig. 1).
4. The production rates (intensities) of the two processes must be the same.

The process of designing polarization-entangled states from two concurrent nonlinear interactions is therefore closely related to the choice of nonlinear interaction geometries, in combination with the physical parameters of the selected nonlinear medium.

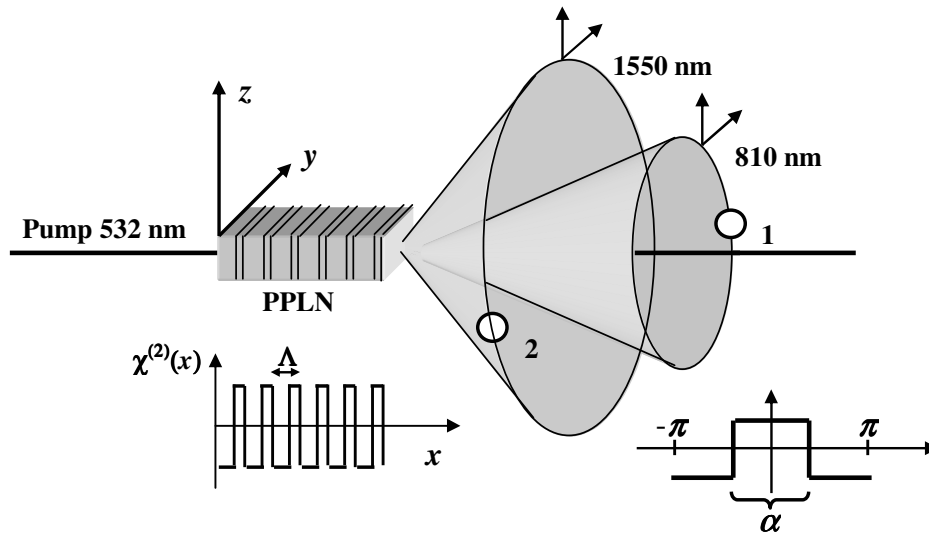


Fig. 1. Principle of generating polarization-entangled pairs at 810 and 1550 nm. Two systems of cones (e and o polarized) are caused to overlap. Entangled pairs are collected along the directions labeled 1 and 2, always on opposite sides of the pump beam. The two inserts illustrate the definitions of the fundamental parameters of the PPC: the period Λ and the (angular) duty cycle α .

2.2. Selection of physical parameters

The production of entangled states of the type $(|e, e\rangle + e^{i\phi}|o, o\rangle)/\sqrt{2}$ is particularly interesting because it can be achieved by the direct overlap of two type-I interactions. As indicated above, this avoids the necessity of birefringent compensation following the crystal [19], and results in a more compact source of entangled photons. In particular, we consider 810 and 1550 nm photons produced by SPDC with a monochromatic laser pump at 532. This choice is motivated by the fact that QKD implementations with both photons at 1550 nm are particularly difficult to realize [27], principally because of the poor efficiency of existing InGaAs single-photon detectors at this wavelength. Because of the technological maturity of Si single-photon detectors in the visible spectrum, in contrast, a hybrid 810/1550 nm configuration can provide a good alternative, provided that the distance traveled in the fiber by the 810-nm photon is sufficiently short [16].

With respect to the material, periodically poled lithium niobate (PPLN) has proven to be an efficient and versatile choice for realizing quasi-phase matching in the context of a nonlinear three-wave mixing process. A numerical simulation was carried out to determine the parameters (spatial pitch and duty cycle) of the PPLN crystal suitable for satisfying the four requirements set forth earlier. A practical and feasible PPLN crystal design is achieved with a spatial pitch $\Lambda = 27.5 \mu\text{m}$ and angular duty cycle 33° (see Fig. 1). In this case, the emission directions of the pair from the $e \rightarrow e + e$ interaction, phase-matched with the fourth order of the nonlinear grating, are coincident with the emission directions of the pair from the $e \rightarrow o + o$ interaction, phase-matched with the zeroth order of the poling period. Zeroth order signifies that the interaction is made possible by natural bulk birefringent phase-matching in lithium niobate.

Exploiting the temperature dependence of the Sellmeier equations for lithium niobate leads to

scattering angles for e -polarized 810 nm and 1550 nm photons (which are, in general, different) that coincide with the angles of corresponding o -polarized 810 nm and 1550 nm photons at 100°C (see Fig. 1). The reduced duty cycle of the poling enables the equalization of the pair production rates for the two participating interactions, since the nonlinear coefficient associated with the first interaction ($d_{33} = 16\text{ pm/V}$) is substantially larger than the coefficient associated with the second interaction ($d_{31} = 2.9\text{ pm/V}$).

2.3. Amplitude and phase of the two-photon state

To simplify the calculation of the two-photon entangled state generated in the previously defined configuration, we restrict our consideration to wavevectors produced in the x - y plane. Since the interior angles between the signal and idler wavevectors, and the direction of the pump (*i.e.* the x axis), are small (2.6° and 5° , respectively), we make use of a paraxial approximation that enables us to eliminate the transverse dependence of the wavevectors. A more complete description of the SPDC phase-matching parameters that includes the transverse behavior of the wavevectors in a strongly non-collinear geometry can indeed be provided by using a methodology described elsewhere [28].

In the simplified case considered here, however, the two-photon state produced in the x - y plane by the $e \rightarrow e + e$ interaction can be written as

$$|\psi_{ee}^{(2)}\rangle \sim \int d\omega_s d\omega_p \delta(\omega_p - \omega_s - \omega_i) \times \quad (10)$$

$$\frac{\tilde{\chi}_{eee}^{(2)}(4q_0)}{\sqrt{n_e(\omega_p)n_e(\omega_s)n_e(\omega_i)}} \int_0^L dx e^{i(k_e(\omega_p) - k_e(\omega_s) - k_e(\omega_i) - 4q_0)x} |1_{\omega_s, \mathbf{k}_e(\omega_s)}\rangle |1_{\omega_i, \mathbf{k}_e(\omega_i)}\rangle.$$

We choose to spread the signal and idler frequencies around their central values ω_s^0 and ω_i^0 , corresponding to the wavelengths of 810 and 1550 nm, respectively. Energy conservation allows us to write $\omega_s = \omega_s^0 + \nu$ and $\omega_i = \omega_i^0 - \nu$. The wavevectors are then $k_e(\omega_s) = k_e(\omega_s^0) + \nu/u_{s,e}$ and $k_e(\omega_i) = k_e(\omega_i^0) - \nu/u_{i,e}$, where $u_{s,e}$ and $u_{i,e}$ are the group velocities for the e -polarization waves at 810 nm and 1550 nm in the PPLN crystal, respectively. Because the quasi-phase matching condition is simply $k_e(\omega_p) - k_e^0(\omega_s) - k_e^0(\omega_i) = 4q_0$, the two-photon state becomes

$$|\psi_{ee}^{(2)}\rangle \sim \frac{\tilde{\chi}_{eee}^{(2)}(4q_0)}{\sqrt{n_e(\omega_p)n_e(\omega_s^0)n_e(\omega_i^0)}} \int_0^L dx e^{-i(1/u_{s,e} - 1/u_{i,e})\nu \cdot x} |1_{\omega_s, \mathbf{k}_e(\omega_s)}\rangle |1_{\omega_i, \mathbf{k}_e(\omega_i)}\rangle. \quad (11)$$

Writing $D_{ee} = 1/u_{s,e} - 1/u_{i,e}$, the integration leads to

$$|\psi_{ee}^{(2)}\rangle \sim -\frac{1}{L} \frac{\tilde{\chi}_{eee}^{(2)}(4q_0)}{\sqrt{n_e(\omega_p)n_e(\omega_s^0)n_e(\omega_i^0)}} e^{-i\nu D_{ee}L/2} \text{sinc}(\nu D_{ee}L/2) |1_{\omega_s, \mathbf{k}_e(\omega_s)}\rangle |1_{\omega_i, \mathbf{k}_e(\omega_i)}\rangle. \quad (12)$$

Similarly, taking $D_{oo} = 1/u_{s,o} - 1/u_{i,o}$, the two-photon state produced by the $e \rightarrow o + o$ interaction is

$$|\psi_{oo}^{(2)}\rangle \sim -\frac{1}{L} \frac{\tilde{\chi}_{ooo}^{(2)}(0)}{\sqrt{n_e(\omega_p)n_o(\omega_s^0)n_o(\omega_i^0)}} e^{-i\nu D_{oo}L/2} \text{sinc}(\nu D_{oo}L/2) |1_{\omega_s, \mathbf{k}_o(\omega_s)}\rangle |1_{\omega_i, \mathbf{k}_o(\omega_i)}\rangle. \quad (13)$$

The state incorporating both pairs [Eq. (8)] is maximally entangled if contributions from both nonlinear processes are totally indistinguishable over their spectral bandwidths:

$$\left| \frac{\tilde{\chi}_{eee}^{(2)}(4q_0)}{\sqrt{n_e(\omega_p)n_e(\omega_s^0)n_e(\omega_i^0)}} \text{sinc}(\nu D_{ee}L/2) \right| = \left| \frac{\tilde{\chi}_{ooo}^{(2)}(0)}{\sqrt{n_e(\omega_p)n_o(\omega_s^0)n_o(\omega_i^0)}} \text{sinc}(\nu D_{oo}L/2) \right|. \quad (14)$$

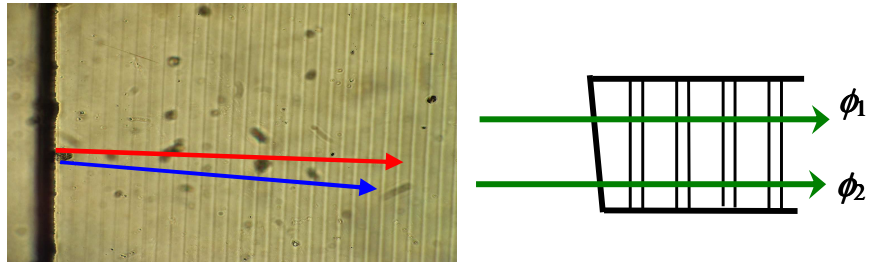


Fig. 2. Left: input face of the poled crystal. The spatial period is $27.5 \mu\text{m}$. Note the highly unbalanced duty cycle between the ferroelectric domains. The red arrow represents the normal to the input face while the blue arrow is the normal to the domain walls. Right: the two-photon state phase ϕ is modified by simply changing the transverse position of the input beam.

The accuracy of this indistinguishability requirement can be estimated by constructing an overlap integral of these two functions over v . In the case of an 8-mm-long PPLN crystal, the agreement is close to 95%. Under these conditions, the necessity of using birefringent compensation following the crystal is essentially obviated, in contrast to the situation for type-II-based SPDC sources. Introducing the notation

$$\tilde{\chi}'_{psi}(q) = \frac{\tilde{\chi}_{psi}^{(2)}(q)}{\sqrt{n_p(\omega_p) n_s(\omega_s^0) n_i(\omega_i^0)}}, \quad (15)$$

the equality of the pair-production rates is readily expressed as $|\tilde{\chi}'_{eee}(4q_0)| = |\tilde{\chi}'_{eoo}(0)|$.

The phase between the two processes that contribute to the joint two-photon entangled state is determined to be

$$\phi = -v(D_{ee} - D_{oo})L/2 + \arg[\tilde{\chi}'_{eee}(4q_0) - \tilde{\chi}'_{eoo}(0)]. \quad (16)$$

For the 8-mm-long PPLN crystal, the variation of the phase arising from frequency dispersion within the spectral width of the signal and idler waves is found to be negligible. For a 2 nm-bandwidth signal, the phase change is estimated to be less than 0.13 rad. Thus the first frequency-dependent term in Eq. (16) is essentially zero. (Note that this discussion is not necessary for the degenerate case of equal signal and idler central frequencies.) Hence, the phase of the two-photon state is governed principally by the second term in Eq. (16), $\arg[\tilde{\chi}'_{eee}(4q_0) - \tilde{\chi}'_{eoo}(0)]$, which is directly linked to the phase properties and spatial profile of the periodically modulated nonlinearity in the poled crystal. In the special case when one of the pairs is generated via harmonic zero (bulk phase matching without modulation), the phase of the entangled state depends solely on the relative position of the rectangular poling structure within the nonlinear crystal. A straightforward and direct way to tune the output state is then to shift the relative phase ϕ by translating a wedged sample perpendicular to the field of the pump beam, as depicted in Fig. 2. This highlights another advantage of generating entanglement using PPCs: the entangled state structure can be easily controlled because it is governed only by the intrinsic properties of the poled crystal.

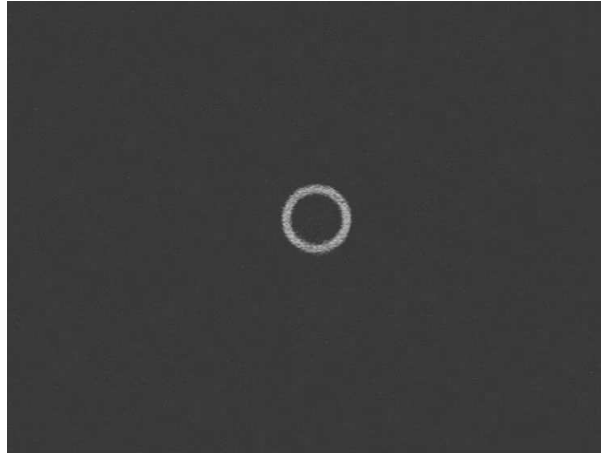


Fig. 3. Movie size: 350 K. Image from the CCD camera that collects the 810-nm SPDC rings as crystal temperature is varied. The bandwidth of the interference filter is 10 nm. The ring that disappears at 130° C is the extraordinary polarized one. The movie illustrates the versatility of using periodically poled structures for applications that exploit non-collinear geometries.

3. Experiment

3.1. Poling of the crystal

We developed procedures and an experimental protocol for poling lithium niobate crystals. A *z*-cut 0.5-mm-thick lithium niobate sample (1" × 1") is patterned with a 3 μ m-thick photoresist layer (Shipley 1813) using standard lithographic techniques. The photomask pattern consists of a rectangular grating with a 27.5- μ m period. The angular duty cycle of the pattern is 25°, leading to 2 μ m-wide openings in the resist. This value is selected to be smaller than the theoretical value (33°), in anticipation of domain spreading during poling. The boundaries of the grating are oriented along the *y*-axis of the lithium-niobate crystal. The length of the grating is 12 mm and its width is 5 mm. A 20-nm-thick layer of nickel-chromium is deposited by e-beam evaporation atop the photoresist pattern to improve nucleation during the poling process, as well as the homogeneity of the domains [29]. The crystal is then inserted in a poling chamber filled with liquid electrolyte (a saturated solution of LiCl), and a high-voltage pulse is applied for a duration of 60 msec to flip the domains. After the poling, the sample is cut to a size 8 × 5 mm and its sides are polished. The input edge is polished at a slight angle with respect to the domains to enable the phase of the two-photon state to be altered by a simple translation of the crystal in the pump beam, in accordance with the illustration provided in Fig. 2.

3.2. Characterization of the parametric downconversion

We characterize the spatial and spectral properties of SPDC by pumping the PPLN crystal with an *e*-polarized, 150-mW, frequency-doubled CW Nd:YAG laser beam that is slightly focused at the center of our sample by means of a 400-mm focal length lens. The PPLN crystal is mounted in an oven with an adjustable temperature between 25 and 230° C. The crystal temperature serves to fine tune the SPDC output. To facilitate the direct observation of SPDC, a collection lens ($f = 38$ mm) is placed at distance f from the crystal. A dichroic mirror and a long-pass filter remove the residual 532-nm pump light, and the SPDC beam is sent through a 810-nm

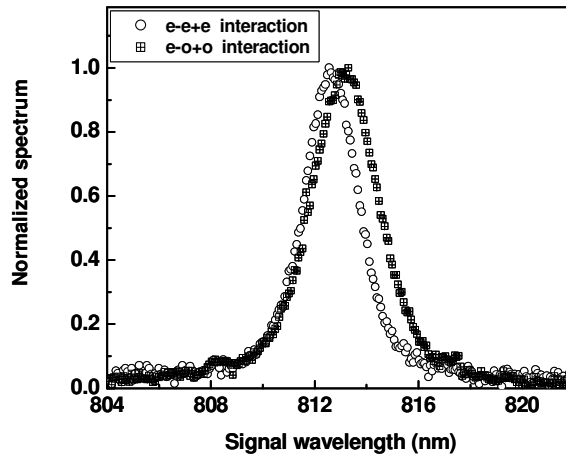


Fig. 4. Relative spectra of the 810-nm photons for the two processes ($e \rightarrow e + e$ and $e \rightarrow o + o$) collected through a narrow pinhole that serves as a spatial filter (see text for details).

interference filter ($\Delta\lambda = 10$ nm). A polarization analyzer allows the polarization of the outgoing photons to be adjusted. A telescope comprising two lenses reduces the size of the beam so that the 810-nm photons suitably impinge on a commercial uncooled silicon CCD camera.

The temperature-dependent SPDC pattern at 810 nm is displayed in Fig. 3. At 60° C, the rings representing the two processes are seen to overlap. The crystal was initially designed to achieve overlap at 100° C; the discrepancy likely arises from the difference between the temperature-dependent Sellmeier coefficients quoted in the literature and those for the actual sample used in our experiments. As the temperature is increased, the diameter of the e -polarized pattern decreases dramatically while the o -polarized pattern changes far less. This asymmetry is a result of the fact that the phase-matching condition for the $e \rightarrow e + e$ interaction is substantially more sensitive to temperature than is that for the $e \rightarrow o + o$ interaction.

To compare the relative intensities of the orthogonally polarized 810-nm beams from the two interactions, we direct all emitted photons to a photodiode surface using a $2f-2f$ configuration. The intensity of the pump beam is ramped up to 750 mW and the analyzer is successively set along the e and o directions. Following a 10-nm-wide interference filter centered at 810 nm, the optical power was observed to be 90 ± 10 nW in both cases, revealing a similar pair-production rate from both interactions.

To evaluate the degree of spectral overlap for the spatially overlapping photons from the two interactions, a 0.5-mm-diameter pinhole is placed at the center of the 810-nm beam, at a distance of 50 cm from the crystal. The beam is then sent to a spectrometer coupled to a cooled CCD camera, which records the spectra. The normalized spectra for both polarizations are presented in Fig. 4. They display significant overlap, although the full-width half-maxima (FWHM) differ slightly as a result of the differing bandwidths of the two interactions. This partial spectral distinguishability can potentially lead to a degradation of entanglement. However, this can likely be obviated by modifying the poling design.

3.3. Bell-state measurement and phase tuning

To demonstrate the nonclassical behavior of the polarization-entangled two-photon state, we carry out a Bell-state measurement using the experimental arrangement schematized in Fig. 5.

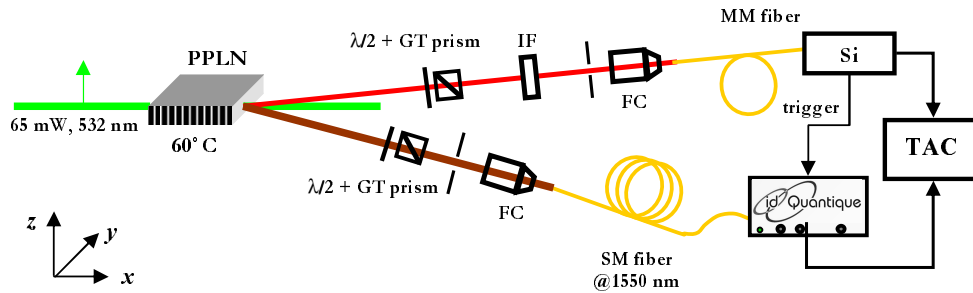


Fig. 5. Experimental arrangement for the Bell-state measurement. IF = interference filter at 810 nm (FWHM = 10 nm), $\lambda/2$ = half-waveplate, GT = Glan-Thompson prism, FC = fiber coupler, MM = multimode, SM = single-mode, Si = silicon APD photon-counting module, idQuantique = InGaAs photon-counting detector, TAC = time-to-amplitude converter.

The intensity of the 532-nm pump beam is reduced to 65 mW and the beam waist is narrowed to $100\ \mu\text{m}$ to enable observation of the change of phase when the crystal is translated in the pump beam. After passing through a $\lambda/2$ -waveplate, a Glan-Thompson prism, and a 10-nm-bandwidth filter centered at 810 nm, the photons are coupled into a multimode fiber that leads to a passively quenched Si single-photon counting module (Perkin-Elmer). The pinhole provides spatial selection for the 810 nm photons. The 1550-nm photons are collected through a similar system (half-wave plate, Glan-Thompson prism and pinhole) and are coupled into a single-mode telecommunications-wavelength fiber. This fiber leads to an InGaAs single-photon counting detector (idQuantique), which, in turn, is triggered by the Si detector. A coincidence circuit based on a time-to-amplitude converter and a multichannel analyzer monitors the coincidence rate. A Bell-state measurement is performed using half-wave plates to select the required polarization projections.

The observed experimental results are presented in Fig. 6. From the number of single counts at 810 nm and from the quantum efficiency of the Silicon avalanche photodiode (about 80%), we can estimate a pair production close to 10^8 pairs/nm bandwidth/sec/steradian per mW of pump. It is apparent from this figure that the singles rate at 810 nm is rather flat (within $\approx 3\%$) indicating a well-balanced presence of both polarizations in the channel. However the coincidence rate is slightly higher when the 1550-nm analyzer is in the horizontal position *-i.e.* along y - (triangles) rather than in the vertical position *-i.e.* along z - (squares). This indicates a greater collection efficiency for the 1550-nm photons from the $e \rightarrow o + o$ interaction than from the $e \rightarrow e + e$ interaction. When the 1550-nm analyzer is set at 45° (circles), the coincidence rate exhibits modulation with a visibility of 75% as the 810-nm waveplate is rotated. This value is larger than the usual Bell-threshold of 70.7% and is sufficient for demonstrating the nonclassical nature of the two-photon polarization state. However, the contributions from the two concurrent type-I nonlinear interactions must be further equalized before this source can be used in a practical QKD setting. We estimate the modification of visibility arising from the intensity mismatch of the nonlinear processes to be approximately 85%. The spectral mismatch also contributes to the degradation of the purity of the state.

To demonstrate the tunability of the entanglement source, we set both analyzers at 45° and record the rate of coincidence as the PPLN crystal is translated perpendicularly to the pump beam. The results are illustrated in Fig. 7. The coincidence rate changes from a maximum to a minimum, demonstrating that the phase ϕ varies from 0 to π . The two-photon entangled state

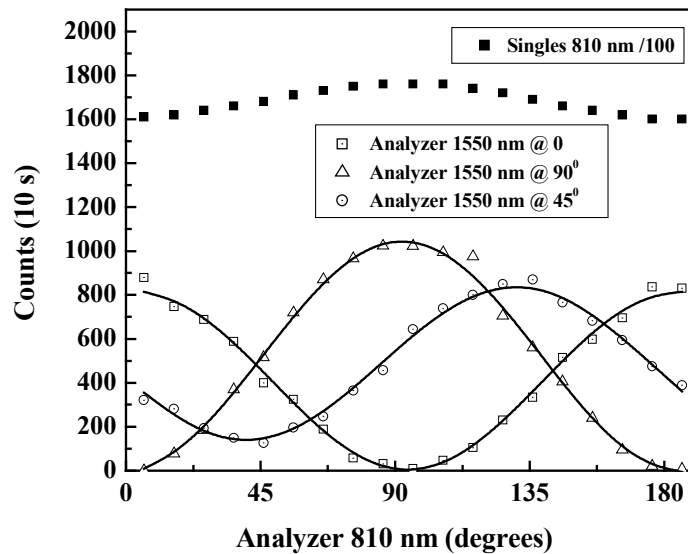


Fig. 6. Results of a Bell-state measurement. Top: singles rate at 810 nm as a function of the orientation of the polarization analyzer in the 810-nm path with respect to the z axis. Bottom: coincidence rates for three different settings of the 1550-nm analyzer.

is effectively adjusted from $\Phi^+ = (|e,e\rangle + |o,o\rangle)/\sqrt{2}$ to $\Phi^- = (|e,e\rangle - |o,o\rangle)/\sqrt{2}$ with a translational shift of $\approx 200 \mu\text{m}$. This clearly demonstrates the ability to tune the phase of an outgoing entangled state by modulating the physical properties of the nonlinear poling pattern in PPLN. Note that the visibility of the two-photon interference could be improved by decreasing the wedge angle of the nonlinear crystal: a substantial loss in the visibility (close to 85%) of the two-photon interference results from the convolution of the pump beam (waist = $100 \mu\text{m}$) with the transverse profile (*i.e.* along y) of the nonlinear pattern ($400 \mu\text{m}$ period).

4. Conclusion

We have carried out a theoretical and experimental study of non-collinear and non-degenerate optical parametric down conversion in a periodically poled lithium niobate crystal, demonstrating the feasibility of constructing a compact source of two-photon polarization entanglement in the 810–1550-nm spectral regions. A specially designed nonlinear poling pattern enables the overlap of two concurrent type-I down conversion interactions in a single PPLN crystal in such a way that pairs of alternatively polarized photons become indistinguishable and thereby contribute coherently to the formation of a two-photon polarization-entangled state. This approach eliminates the traditional external compensation optics. We showed further that the phase of the ensuing entangled state can be continuously adjusted by simply translating the nonlinear crystal relative to the pump beam.

Although this first experimental test of entangled-state production using two concurrent type-I nonlinear interactions in a PPLN crystal is most promising, a number of improvements must be effected before it can be adopted for use in a practical QKD implementation. The design of the periodically poled crystal can be improved quite easily: reducing the crystal length should

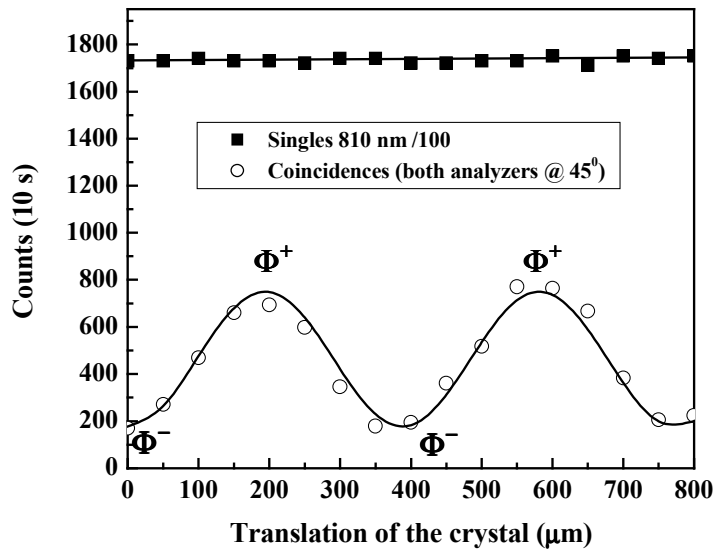


Fig. 7. Demonstration of the tunability of the output two-photon state. Both analyzers are set at 45° and the crystal is translated perpendicularly to the pump beam. Top: singles rate at 810 nm. Bottom: coincidence rate. The translation distances at which Φ^+ and Φ^- emerge are shown.

ameliorate the spectral mismatch between the two nonlinear contributions, and a wider poled pattern relative to the pump beam waist should lead to a higher degree of entanglement. Finally, it will be useful to more accurately control the duty cycle of the nonlinear profile to better equalize pair production and to enhance the coherence of the state. The symmetry of collecting the 1550 nm photons can be improved by modifying the fiber-coupling optics.

We believe that our results demonstrate a significant potential for periodically poled crystals with specially designed patterns as sources of entanglement. The possibilities offered by multiple concurring nonlinear interactions offer a roadmap for the implementation of compact, sophisticated devices. The approach set forth here can be extended, for example, to the design and construction of bidimensional nonlinear PPLN structures that allow direct access to the simultaneous manipulation of polarization and frequency entanglement [30].

Acknowledgments

This work was supported by a U.S. Army Research Office (ARO) Multidisciplinary University Research Initiative (MURI); by the Center for Subsurface Sensing and Imaging Systems (CenSSIS), an NSF Engineering Research Center; by the National Science Foundation (NSF); by the Defense Advanced Research Projects Agency (DARPA); and by the David & Lucile Packard Foundation. G.D.G. also acknowledges financial support from the Ministero della Istruzione, dell' Università e della Ricerca (PRIN-2005024254 and FIRB-RBAU01L5AZ) and the European Commission through the Integrated Project "Qubit Applications" (QAP), contract No. 015848, funded by the IST directorat.